Final Design, Manufacturing and Testing of the Clean Sky 2 Distributed Electric Propulsion Scaled Flight Demonstrator D08 DEP-SFD

Döll, Carsten; Hoogreef, M.F.M.; Iannelli, Pierluigi

DOI
10.2514/6.2024-1304

Publication date
2024

Document Version
Final published version

Published in
Proceedings of the AIAA SCITECH 2024 Forum

AIAA SciTech Forum
8-12 January 2024, Orlando, FL
AIAA SCITECH 2024 Forum

10.2514/6.2024-1304

Final Design, Manufacturing and Testing of the Clean Sky 2 Distributed Electric Propulsion Scaled Flight Demonstrator D08 DEP–SFD

Carsten Döll *
ONERA / DTIS, University of Toulouse, Toulouse, F-31055, France

Maurice F.M. Hoogreef †
TU Delft / Faculty of Aerospace Engineering, Delft, NL-2629HS, The Netherlands

Pierluigi Iannelli ‡
CIRA / Fluid Dynamics Department, Capua, I-81043, Italy

Henk Jentink §
NLR, Amsterdam, NL-1006BM, The Netherlands

Daniel Kierbel ¶
Airbus, Toulouse, F-31027, France

Within the work package radical new aircraft configuration of Cleansky2 Large Passenger Aircraft, a benefit of more than 20% in fuel consumption and CO2 emission (one of CS2 top level objectives) could be achieved by using various Distributed (hybrid) Electric Propulsion DEP architectures on different more or less radical aircraft configurations. It has therefore been identified as a disruptive technology which shall be de-risked in terms of achievable performance during wind tunnel tests and in terms of handling qualities during flight tests. The electric architecture with typical magnitudes shall also be studied in more detail. As already presented during AIAA SciTech Forum and Exhibition 2023, the D08 Distributed Electric Propulsion DEP version of the D03 Scaled Flight Demonstrator has been designed, manufactured and ground tested from 2020 to May 2023. An incident during the last ground test in May 2023 caused the total loss of this demonstrator. After its analysis, it was decided to robustify the electric architecture by improving the batteries, the wiring, the protections and the monitoring. These changes in the electric architectures lead to structural changes like the shift of the emergency parachute and bigger access hatches. The remanufacturing of the DEP-SFD2 has started in September 2023 for an exhaustive integration test campaign and taxi tests in January and February 2024. At the moment, the qualification flight tests will take place in April 2024 and the mission flight tests in May 2024.

I. Introduction

Within the WP1.6.1 of the Joint Undertaking JU Clean Sky2, different radical configurations have been studied by DLR, ONERA, NLR and TU Delft until end of 2019 in order to contribute to the top level

*Research Scientist, Information Processing and Systems, 2, Carsten.Doll@onera.fr
†Assistant Professor, Flight Performance and Propulsion, M.F.M.Hoogreef@tudelft.nl
‡Research Scientist, Fluid Dynamics, P.Iannelli@cira.it
§Research Scientist, Systems, Henk.Jentink@nlr.nl
¶Project Manager, Future projects, Daniel.Kierbel@airbus.com

objective of Clean Sky2 of a 20% block fuel reduction at Entry in Service EIS in 2035 with respect to a reference passenger transport aircraft of 2014 as shown on Fig. I. DLR[1] studied a configuration with boosted turbofan, with boundary layer ingestion fans at the rear fuselage or at the wing tip or with a canard configuration. This top level objective is not fully reached. However, these studies continued within the German national research program SYNERGY.

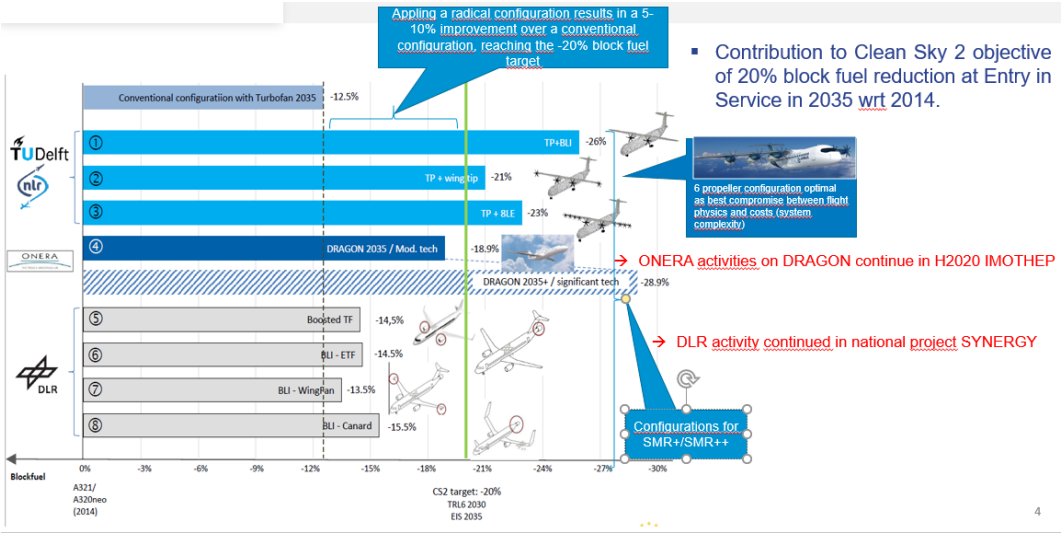

Figure 1. The different suggested radical configurations with respect to the 20% block fuel reduction top level objective of Clean Sky 2

ONERA[2–4] studied the hybrid electric DRAGON concept for Mach 0.7 with 2 classical fuel burning turboshafts as generators at the rear fuselage and with 24 distributed ducted electric fans installed under the trailing wing edge. The main design driver was to improve the overall propulsive efficiency of this transonic A/C by increasing virtually its global By Pass Ratio BPR thanks to the distribution of small fans while being able to integrate them without creating shocks and while ensuring high level reliability constraints. The overall propulsive efficiency of this hybrid electric concept depends on the virtual BPR of the ducted fans, on the efficiency of the electric architecure (wiring, converters, power electronics, generators, ...) and the turboshaft efficiency. At that time, it has been shown that a virtual BPR ≈ 50 with small fan diameters can be reached which is about 3 times the BPRs of the actual Ultra High By Pass Ratio UHBPR engines with large fan diameters. The electric architecture has been sized with off-the-shell components. The 2 turboshafts have been sized such that they operate in optimal conditions to generate a maximum of electricity. The resulting A/C could reach more than 20% of block fuel reduction. This promising result led to the launch the European project H2020 IMOTHEP where the significant increase of the virtual BPR and the efficiency of the electric architecture could be confirmed. However, the turboshaft design has been identified as a key design bottle-neck. Engine manufacturers have sized this critical element and its resulting efficiency is much less than the one predicted by ONERA. The overall DRAGON efficiency is therefore much less than the one shown on Fig. I.

NLR and TU Delft[5] studied various propeller driven configurations with different number of engines. They reach the top level objective thanks to speed reduction (about 10% of block fuel reduction) and thanks to the slipstream effect created by distributed electric propulsion (also about 10% of block fuel reduction). Based on off-the-shelf available technology, an expected entry in service EIS by 2035 of these configurations is also more likely than for above DRAGON concept. While NASA[6] worked on the X-57 Maxwell concept of a general aviation aircraft with 14 engines searching for an aerodynamic optimum, here the partners have selected a 6 electric driven propeller configuration as the best compromise between flight physics, costs and system complexity for de-risking the disruptive technology 'Distributed Electric Propulsion DEP'in terms of achievable performances during wind tunnel tests and in terms of handling qualities during flight tests.

II. Initial Design, Manufacturing and Testing

This section recalls the initial design, manufacturing[7] and testing[8] process of the D08 Distributed Electric Propulsion–Scaled Flight Demonstrator DEP-SFD.

A. Design

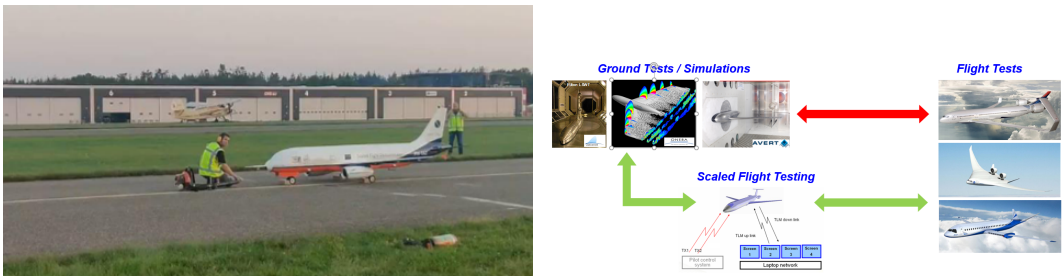

Figure 2. The Scaled Flight Demonstrator SFD D03.

The D03 Scaled Flight Demonstrator SFD is depicted on the left of Fig. 2 just before its first flight. It was developed within WP1.3 during Clean Sky2 in order to demonstrate the interest of scaled flight testing as a complementary mean for testing mainly the dynamic behaviour of new (radical) A/C configurations during flight in addition to numerical simulations, ground component and windtunnel tests at a very early design stage well before starting the manufacturing of the first real size prototype. The idea is illustrated on the right of Fig. 2.

As the main objective of scaled flight demonstration is the dynamic behaviour, the so-called Froude Scaling has to be applied instead of the widely used Reynolds Scaling for windtunnel tests, which scales the geometry and the inertia of the demonstrator such that the reference transport aircraft at different reference flight conditions is well represented at the chosen test flight conditions at about Mach 0.4 at low altitude. The selected scale is 1/8.5, *i.e.* the wing span $b = 4m$ for a maximum take-off weight $MTOW = 140kg$. The concept of scaled flight demonstration[9,10] has been validated.

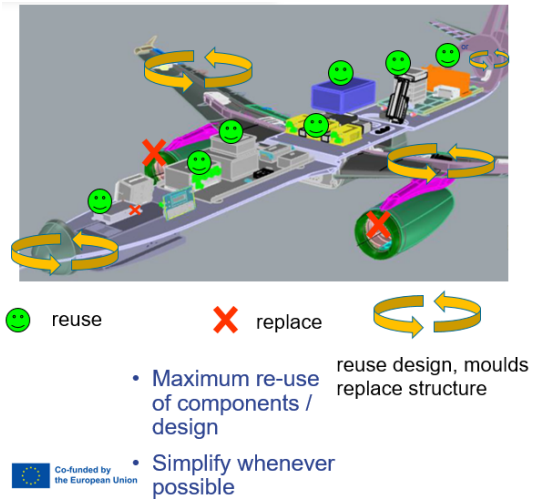

Figure 3. The design philosophy for the D08 DEP-SFD.

The main design driver for the D08 Distributed Electric Propulsion–Scaled Flight Demonstrator DEP-SFD was to de-risk the key technology Distributed Electric Propulsion mainly in terms of dynamics and control by modifying the above D03 SFD with minimal development costs. For that reason, its design,

moulds and components are re-used as much as possible while simplifying whenever it was possible. 106 parts of the 124 parts of the D03 could be re-used for the D08 where 65 are identically remanufactured components and 25 are taken directly from the D03 after its flight campaign and re-employed on the D08, such as the landing gear and the main flight test instrumentation FTI. 18 parts could be omitted and 35 parts had to be specifically be designed, namely the hexa-engine controller HEC, the 6 engine speed controllers ESC, the 6 electric engines and propellers as well as the battery system and the electric wiring. This design philosophy shown on Fig. 3 has been followed by NLR, TU Delft and OrangeAerospace during the feasibility study until September 2020 and the conceptual design phase until December 2020.

During the preliminary design phase until April 2021, the location of the 6 engines and the 6 propeller diameters have been frozen by aerodynamic CFD computations in order to maximize the slipstream effect while reducing drag as much as possible. The 6 blade propellers are based on the XPROP design of TU Delft. The tip engines have smaller propellers for a bigger ground clearance during cross-wind landings, see Fig. 4. Another advantage of this installation is that the tip engines need less power than the inner and middle engines while producing the same thrust. These engines will therefore be smaller and lighter, which has also a positive effect on the wing bending and the structural sizing of the wing. The electric power of one engine has been evaluated by $4kW$ at a nominal voltage of 44.4V. The electric capacity was initially covered by 4 packs of Lithium Polymer LiPo batteries.

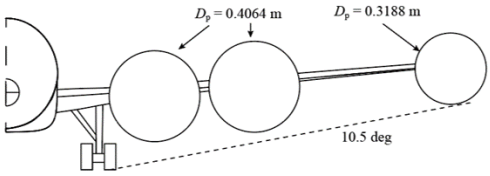

Figure 4. The 6 engine positions and propeller diameters.

The final design phase was conducted until November 2021 by NLR, TU Delft and OrangeAerospace which confirmed the design choices of earlier stages. Especially, the propeller rotation senses have been frozen and the nacelle design has been fine-tuned by CFD computations in order to improve the flow separation characteristics around the nacelles. The nacelles have slightly be shifted downwards by half the nacelle radius $0.5R_{nacelle}$ and slightly inclined by -3^o as shown on Fig. 5. The electric capacity demand was reevaluated by 6 packs of LiPo batteries.

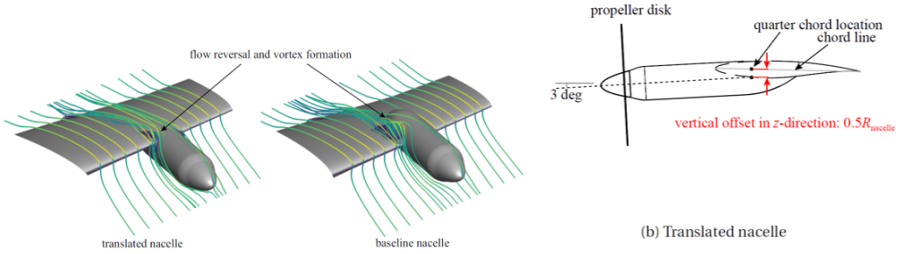

Figure 5. The modified nacelle installation for better flow seperation characteristics.[11]

B. Manufacturing

The manufacturing started in January 2022. Structural parts of the fuselage have been integrated by NLR and OrangeAerospace in April 2022, the wing and the fuselage have been assembled in June 2022 as depicted on Fig. 6. The fully assembled and painted DEP-SFD has been shipped to the windtunnel facilities in December 2022.

Figure 6. Structural parts of the fuselage and the assembly of the wing and the fuselage.

C. Windtunnel tests

The DEP-SFD has been tested in the DNW LLF windtunnel facilities in Marknesse, The Netherlands, on January 2023, 11^{th} and 12^{nd} during about 300 test runs. See Fig. 7 for its installation in the windtunnel.

Figure 7. The DEP–SFD D08 in the DNW windtunnel facilities in Marknesse, The Netherlands.

On Fig. 8, the lift coefficient $C_L(\alpha)$ is plotted in function of the angle of attack α when all engines push the same for three different throttle settings : $dx = 0\%$ in blue, $dx = 47\%$ in red and $dx = 90\%$ in green and for three different flap settings : clean (quadrilateral), take-off (crosses) and landing (triangles). As expected, the lift is a linear function of α until the stall. Thanks to the slipstream effect, the lift gradient is bigger for higher thrust settings, while the stall starts later. With flap settings, the lift is even higher as expected.

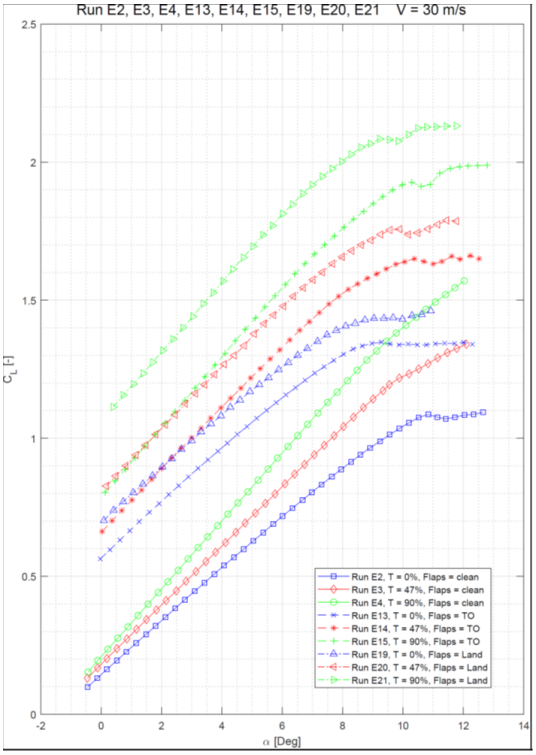

Figure 8. The lift coefficient $C_L(\alpha)$ in function of the angle of attack α for three different throttle settings dx and three different flap settings.

On the left hand of Fig. 9, the yaw moment coefficient $C_n(F)$ is plotted when one of the left engines pushes with more thrust $+dF$ and its corresponding right engine pushes with less thrust $-dF$. As expected,

the yawing moment created by the most left engine, *i.e.* the left tip propeller LTP (green), is the biggest one thanks to its big lever arm with respect to the centre of gravity CG, the yawing moment created by the inner left engine, *i.e.* the left inner propeller LIP (blue), is the smallest one due to its small lever arm. Also as expected, the bigger the thrust variation dF, the bigger is the created yawing moment. The green curve is saturated at the maximum thrust value $\max(F+dF)$ of the left engine while the thrust of the corresponding right engine can further be reduced to $F-dF$ creating still more yawing moment.

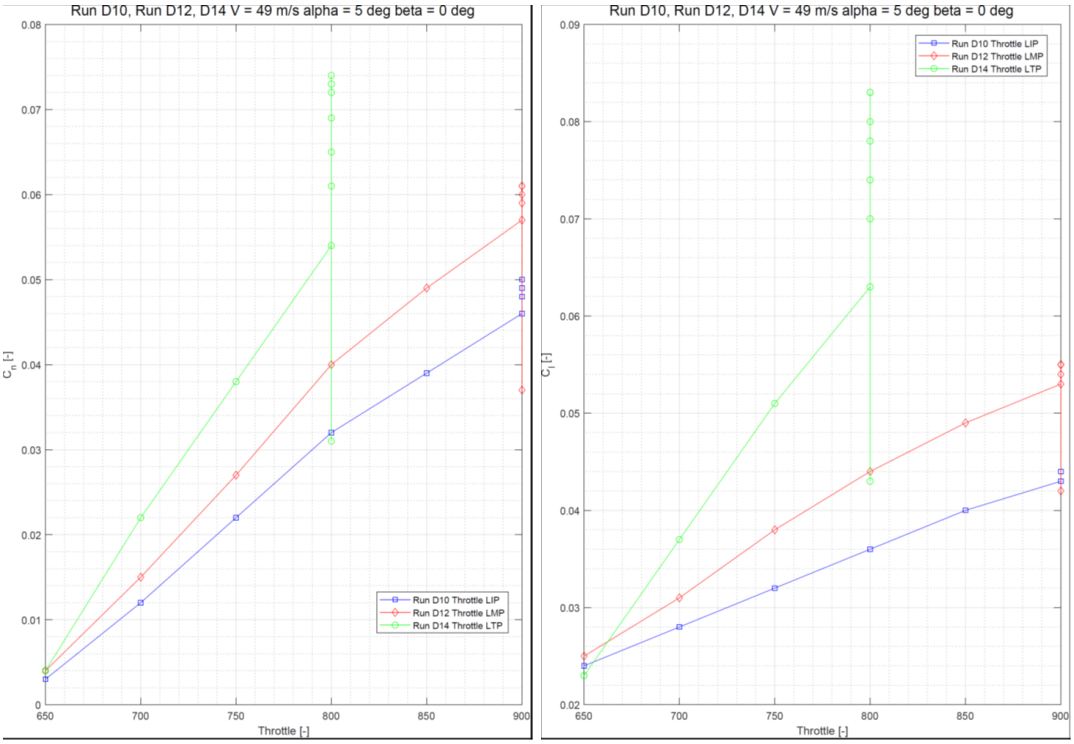

Figure 9. The yaw moment coefficient $C_n(dF)$ and the roll moment coefficient $C_l(dF)$ in function of the thrust variation dF for the three different left engines.

On the right hand of Fig. 9, the roll moment coefficient $C_l(F)$ is plotted when one of the left engines pushes with more thrust $+dF$ and its corresponding right engine pushes with less thrust $-dF$. The rolling moment created by the most left engine LTP is the biggest one (green), the rolling moment created by the inner left engine LIP is the smallest one (blue). The rolling moment is created by the additional lift stemming from the slipstream effect and the corresponding lever arm. The slipstream effect is bigger in the middle part of the wing due to the elliptic lift distribution. The bigger lever arm of the LTP overcompensates the smaller slipstream effect. As expected, the bigger the thrust variation dF, the bigger is the created rolling moment thanks to the larger slipstream effect. The green curve is saturated again at the maximum thrust value $\max(F+dF)$ of the left engine while the thrust of the corresponding right engine can further be reduced to $F-dF$ creating still more rolling moment.

During these windtunnel tests, an higher heating of the tip engines has been monitored than the heating of the middle and inner engines. This is due to their smaller propeller and therefore an higher rotational speed compared to the middle and inner engines for the same thrust. In order to improve the air cooling of these tip engines, air inlets have been added to the tip propeller nacelles.

D. Static ground tests

After the windtunnel tests, typical mission profiles with 5 go-arounds have been simulated during static ground tests in order to observe the available network voltage, the currents and electric power during a whole flight and in order to validate the take-off and landing procedures at Grottaglie Airport, Italy. An higher voltage drop than expected was observed due to battery discharge for the last go-around which would

have led to a longer take-off distance rendering it extremely difficult to stay within the authorized flight zone at the airport. This issue should be monitored during the high speed taxi tests.

E. High speed taxi tests, last static ground test and lessons learnt

The windtunnel tests confirmed the predicted CFD computations for all aerodynamic coefficients which allowed us to proceed with the high speed taxi tests at Deelen Airport, The Netherlands on March, 28^{th} and 29^{th} as shown on Fig. 10.

Figure 10. The DEP-SFD during its high speed taxi tests at Deelen Airport.

These high speed taxi tests confirmed the predicted take-off performances in terms of rotation speed V_1, control of the demonstrator on ground, power needs, current levels and heating of the electric motors and their engine speed controllers ESC. Namely, the added cooling of the tip engines of §C has been validated. However, the higher simulated voltage drop of §D has also been observed at the end of the taxi tests. In order to avoid to change the authorized flight zone at Grottaglie airport, it was decided to replace the initial power batteries by batteries with a higher discharge rating and to add one more battery pack.

With these new batteries, a last static ground test simulating a typical mission profile has been executed on May, 11^{th} which should have validated the overall design in terms of available power, especially during the last go-around. Unfortunately, an incident caused the total loss of the demonstrator. The lessons learnt from this incident are :

- The DEP-SFD was insured with a hull insurance via Airbus thanks to our Joint Ownership Agreement since January 2023.
- The insurance refunded the total amount minus the franchise and some reusable parts following the incident analysis and damage report which allowed us to start robustifying and rebuilding the DEP-SFD2.
- The incident analysis realized between May and August 2023 highlighted the need to robustify the electric architecture of the demonstrator by improving :
  - the batteries,
  - the wiring,
  - the protections and
  - the monitoring

  which also led to the need to :
  - simplify the access to the batteries,
  - separate as much as possible heat sources and
  - increase as much as possible heat exchanges.
- These modifications will also lead to structural design changes, especially on the fuselage.
- It also appeared that extensive tests for all electric components have to be conducted on an iron-bird test bench representing the physical location and environment of the components within the demonstrator.

III. Robustification of the electric architecture

The robustified electric architecture has been approved during a new Critical Design Review on October, 23^{rd}. The main modifications will be presented in this section.

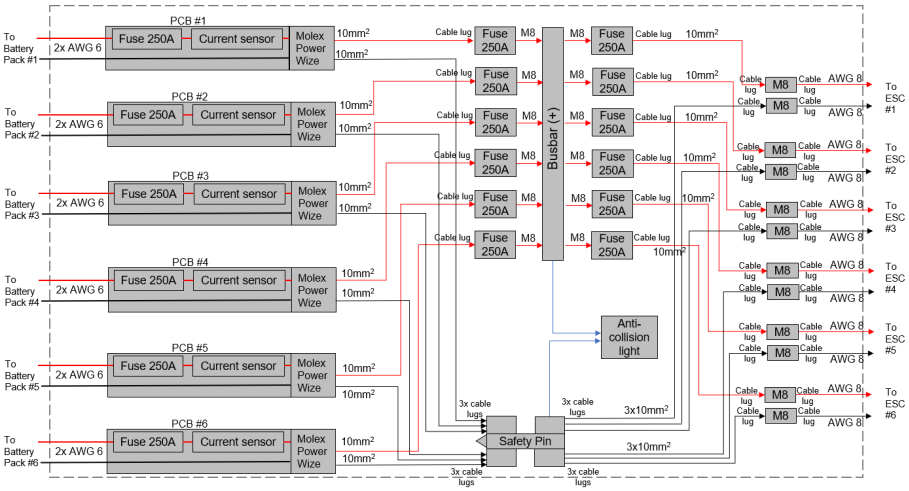

Figure 11. The robustified electric architecture of the DEP–SFD2.

It has been decided to increase the nominal voltage from 44.4V to 51.8V which permits the necessary voltage during the last go-around for a nominal take-off distance even with a voltage drop due to battery discharge. The higher voltage will also decrease the currents on the network for the same power consumption, which will lead to a lower heat production in the cables and components. This higher voltage and the necessary capacity will be delivered by 6 packs of new off-the-shell LiPo batteries with a 30C discharge rating as a baseline solution. One spare battery will be submitted to structural tests in order to gain confidence in the battery housing while all other operational batteries will be submitted to a minimal number of charging and discharging cycles in order to gain confidence in their operational reliability. They will also be extensively tested within the iron-bird environment of §IV for heating monitoring. A second option was studied to replace these off-the-shell baseline batteries by specifically developed ones. Their use is however jeopardized by the timing for their development, manufacturing and testing before the shipping of DEP-SFD2 to Grottaglie planned for the moment being in March 2024.

The robustified electric distribution network from the 6 power batteries to the 6 engine speed controller ESCs is depicted on Fig. 11. 6 red (+) cables run from the 6 batteries to the (+) busbar. Each of these cables in the fuselage is of gauge $10mm^2$ and is protected close to the battery by 1 fuse and monitored by 1 non-intrusive Hall effect current sensor. It is connected to the red (+) cable of an increased gauge AWG6 attached to the battery via a new robustified connector. Close to the (+) busbar an additional fuse is installed on each of these red (+) cables. 6 red (+) cables of gauge $10mm^2$ run from the (+) busbar through the wing to the 6 ESCs connectors of increased size M8. Each of these cables is also protected by a fuse close to the (+) busbar. The red (+) cables attached to the ESC are of gauge AWG8. The black (GND) cables of the ESCs are also of gauge AWG8, are connected to the cables in the wing of gauge $10mm^2$ to the safety pin located at the root of the left wing which acts as (GND) busbar. The latter one is connected to the above mentioned robustified battery connectors via 6 black (GND) cables of gauge $10mm^2$. Between these connectors and the batteries run 6 black (GND) cables attached to the batteries of gauge AWG6. Taking into account the current derating, the 18 fuses have been sized for 250A. If the safety pin is pulled out, it cuts the current between the batteries and the ESCs. It secures the demonstrator.

IV. Final Design, Manufacturing and Testing

In order to simplify the access to the batteries for storing and charging operations, the batteries have been moved forward under the enlarged front hatch as depicted on Fig. 12. This also allowed to increase

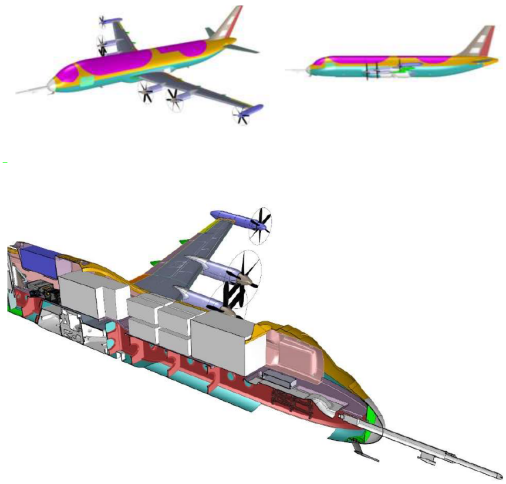

Figure 12. The modified design for the DEP–SFD2.

the available space for the battery packs : More batteries can be installed while offering also more space between the batteries for a better heat exchange thanks to natural airflow. On the contrary, the flight test instrumentation FTI had to be shifted to the rear as well as the emergency parachute which also led to an enlarged rear hatch for the DEP-SFD2. The FTI interface had also to be adapted to the additional measurement signals for the added current, voltage and temperature sensors. However, it is finally smaller and lighter than the original one.

Figure 13. The freshly manufactured fuselage and wings of the DEP–SFD2.

The manufacturing of the modified structural parts like the fuselage and the wings for the DEP-SFD2 started end of August 2023 and was finalized mid-November 2023 as shown on Fig. 13.

In parallel, the iron-bird test bench for the DEP-SFD2 has been built and installed at NLR facilities mid of November 2023. See Fig. 14 during a first test. The cables are for example wired within specific cable trays imitating more severe conditions than the environmental conditions witin the wing. The engines with their ESCs are installed with or without their nacelles. The safety pin is also installed in a specific housing. The (+) busbar is installed in the center of this iron-bird simulating the fuselage. At the beginning, the electricity is delivered by specific external power supplies. In January, the new chosen power batteries will also be tested within this iron-bird.

Figure 14. The iron-bird of the DEP–SFD2.

At the moment, several tests have already been realized concerning mainly the cable sizing within the wings and the choice of the safety pin as well as the choice of the fuses. The temperatures of the cables, the safety pin and the fuses have been measured for nominal mission profiles and for various failure scenarii like short circuits or power source failures on one or several lines. On Fig. 15 are depicted the temperature profiles around the cables within the wing cable tray during a nominal mission flight. The temperature rise during this mission is of about 10K within the cable tray. At the core of the cables this temperature rise is of about 25K. This is well below the maximal allowed nominal operational temperature for cables of gauge $10mm^2$. Their sizing is therefore frozen. The temperature rise during this mission of the safety pin is also below 25K which also validates its design. The wing can therefore be closed soon for starting the final assembly of the DEP-SFD2.

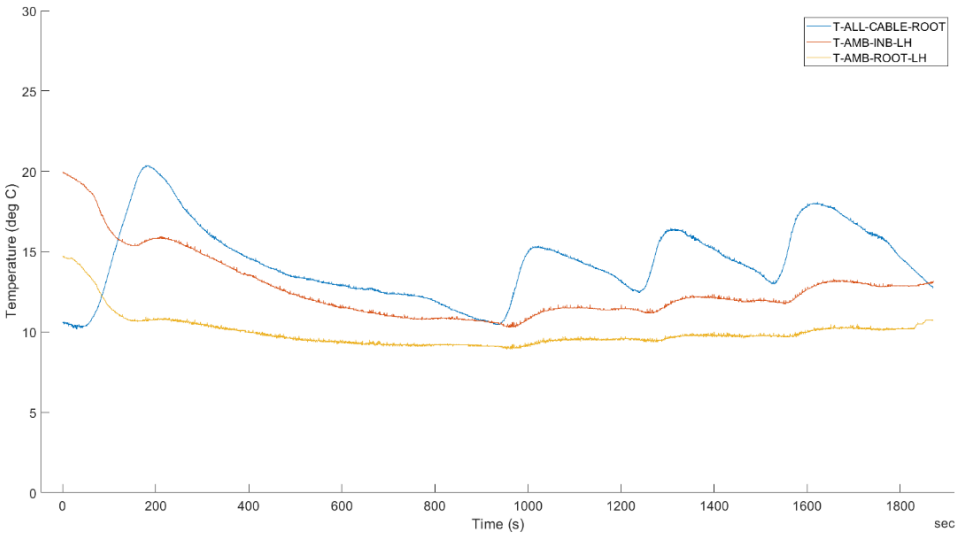

Figure 15. The temperature profiles around the cables within the wing cable tray during a nominal mission flight.

V. Conclusions and Perspectives

An incident during the last ground test in May 2023 caused the total loss of the DEP-SFD demonstrator. After its analysis, it was decided to robustify the electric architecture by improving the batteries, the wiring, the protections and the monitoring. These changes in the electric architectures lead to structural changes like the shift of the emergency parachute and bigger access hatches. The remanufacturing of the DEP-SFD2 has been started in September 2023 for an exhaustive integration test campaign at NLR facilities in the Netherlands in January 2024 and low and high speed taxi tests at Deelen Airport in the Netherlands in February 2024. The DEP-SFD2 will then be shipped to Grottaglie Airport in Italy for its qualification flight tests in April 2024 and its mission flight tests in May-June 2024.

Acknowledgments

This project has received or receive funding from the Clean Sky 2 Joint Undertaking (JU) under grant agreement No 945583. The JU receives support from the European Union's Horizon 2020 research and innovation programme and the Clean Sky 2 JU members other than the Union.

The authors would also like to thank all team members within Airbus, CIRA, NLR, ONERA, OrangeAerospace and TU Delft at demonstrator level as well as all the partners at platform level for fruitful discussions and their investment.

References

[1]Atanasov, G., "Potential Propulsion Architecture for a Reduced Climate Impact of Civil Aviation," *Proc. E2FLIGHT Conference 2020*, Stuttgart, Germany, February 2020.

[2]Döll, C., Nguyen-Van, E., Schmollgruber, P., and Defoort, S., "The status of work on DRAGON : the hybrid Distributed electric propulsion Research Aircraft concept by ONERA," *Proc. E2FLIGHT Conference 2020*, Stuttgart, Germany, February 2020.

[3]Döll, C., Nguyen-Van, E., Schmollgruber, P., and Defoort, S., "Refined Multidisciplinary design and performance of DRAGON (Distributed fans Research Aircraft with electric Generators by ONERA)," *Proc. AIAA SciTech Forum*, Virtual Session, January 2021.

[4]Nguyen-Van, E., Viguier, C., Mezani, S., Sainz, J., Takorabet, N., and Defoort, S., "Design and performances of a Turbo-Electric and Distributed Propulsion aircraft in the Small and Medium Range segment: intermediate results from the European project IMOTHEP," *Proc. AIAA SciTech Forum*, Orlando, Florida, USA, January 2024.

[5]Hoogreef, M., Vos, R., de Vries, R., and Veldhuis, L., "Conceptual Assessment of Hybrid Electric Aircraft with Distributed Propulsion and Boosted Turbofans," *Proc. AIAA SciTech Forum*, San Diego, California, USA, January 2019.

[6]Litherland, B., Borer, N., and Zawodny, N., "X-57 Maxwell High-Lift Propeller Testing and Model Development," *Proc. AIAA Aviation Forum*, Virtual Session, August 2021.

[7]Döll, C., Jentink, H., Iannelli, P., Hoogreef, M., and Kierbel, D., "The D08 Distributed Electric Propulsion Scaled Flight Demonstrator DEP-SFD," *Proc. AIAA SciTech Forum*, National Harbor, Maryland, USA, January 2023.

[8]Döll, C., Jentink, H., Iannelli, P., Hoogreef, M., and Kierbel, D., "Design, manufacturing and testinf of the Clean Sky 2 Distributed Electric Propulsion Scaled Flight Demonstrator D08 DEP-SFD," *Proc. 13th EASN International Conference*, Salerno, Italy, September 2023.

[9]Schmollgruber, P., Toussaint, C., Lepage, A., Bremmers, F., Jentink, H., Timmermans, L., Genito, N., Rispoli, A., Meissner, D., and Kierbel, D., "Validation of scaled flight testing," *Proc. 33rd ICAS Congress*, Stockholm, Sweden, September 2022.

[10]Schmollgruber, P., Jentink, H., Iannelli, P., and Kierbel, D., "The D03 Scaled Flight Demonstrator SFD," *Proc. AIAA SciTech Forum*, National Harbor, Maryland, USA, January 2023.

[11]de Vries, R. and Vos, R., "Aerodynamic Performance Benefits of Over-the-Wing Distributed Propulsion for Hybrid-Electric Transport Aircraft," *AIAA Journal of Aircraft*, Vol. 60, No. 4, April 2023, pp. 1201–1218.